© 2016 IJSRSET | Volume 2 | Issue 4 | Print ISSN : 2395-1990 | Online ISSN : 2394-4099
Themed Section: Engineering and Technology

Analysis of Compressible Effect in the Flow Metering By Orifice Plate Using CFD

Prasanna M A*[1], Dr. V. Seshadri[2], Yogesh Kumar K. J.[3]
[*1]M Tech Student, Thermal Power Engineering, MIT-Mysore, India
[2]Professor (Emeritus), Department of Mechanical Engineering, MIT Mysore, India
[3]Assistant Professor, Department of mechanical engineering, MIT Mysore, India

ABSTRACT

The orifice plate is a typical obstruction type of flow meter, widely used in industries for flow measurement. ISO-5167-1 and BS1042 standards provide the value of Discharge Coefficient for both standard Orifice Plate and Quarter Circle Orifice Plate. In the present work, an attempt is made to study and develop a computational model of flow through an Orifice Plate which can be used as an efficient and easy means for predicting the compressibility effect using Computational Fluid Dynamics (CFD) software. ANSYS FLUENT-14 has been used as a tool to perform the modelling and simulation of flow through Orifice Plate. Analysis of flow through Orifice Plate has demonstrated the capability of the CFD methodology for predicting the accurately the values of C_d, ε and C_{PL} over a wide range of operating conditions. CFD methodology also has been used to analyse the effect of various parameters like diameter ratio, Reynolds number, and pressure ratio on the performance parameters of the orifice meters. It has been demonstrated that the validated CFD methodology can be used to predict the performance parameters of orifice plate assemblies even under conditions not covered by ISO 5167-1 and BS1042 standards.

Keywords: Coefficient of Discharge, Computational Fluid Dynamics, Expansibility Factor, Quarter Circle Orifice Plate, Square Edge Orifice Plate, Permanent Pressure Loss Coefficient.

I. INTRODUCTION

The flow meters are being widely used in the industries to measure the volumetric flow rate of the fluids. These flow meters are usually differential pressure type, which measure the flow rate by introducing a constriction in the flow. The pressure difference caused by the constriction is used to measure the flow rate by using Bernoulli's theorem.

If any constriction is placed in a pipe carrying a fluid, there will be an increase in the velocity and hence the kinetic energy increases at the point of constriction. From the energy balance equation given by Bernoulli's theorem, there must be a corresponding reduction in the static pressure.

Thus by knowing the pressure differential, the density of the fluid, the area available for flow at the constriction and the discharge coefficient, the rate of discharge from the constriction can be calculated. The discharge coefficient (C_d) is the ratio of actual flow to the theoretical flow. The widely used flow meters in the industries are Orifice meter, Venturimeter and Flow Nozzle. Venturimeter and orifice meters are more convenient and frequently used for measuring flow in an enclosed ducts or channels.

The objective of the present work is to study the compressibility effect on different types of the orifice plates such as Standard Concentric Orifice Plate, Quarter Circle Orifice Plate and Square Edge Orifice Plate. The aim of the study is also to demonstrate the capability of the CFD methodology to predict accurately the values of C_d, ε and C_{PL} over a wide range of operating conditions. The performances of these meters in terms of value of discharge coefficient and pressure loss have been investigated by several researchers. Karthik G S et al [1] have predicted the performance characteristics of orifice plate assembly for non standard conditions using CFD, W.B.Brower et al [2] have investigated the compressible flow through an orifice, Karthik G S [3] has made CFD

analysis Flow through orifice plate assemblies used for specialized non standard working conditions, R.Kis et al [4] have reported a CFD analysis of flow through a high pressure natural gas pipeline with an undeformed and deformed orifice plate. It is observed from the above that the compressibility effect in the flow through orifice plates has not been analyzed fully. Hence in the present study CFD has been used to study the effect of compressibility of the fluid on the performance parameters of the orifice meters over a wide range of operating conditions.

Principle of Orifice Plate

The Orifice Plate is an obstruction type flow meter consists of a circular plate at the center cross section as shown in the Fig.1.

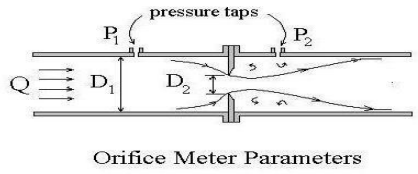

Figure 1: Orifice Plate

The function of the downstream region is to increase the velocity of the fluid and temporarily reduce its static pressure. Thus the pressure difference between the inlet and the vena contracta is developed. This pressure difference is correlated to the rate of flow of fluid by using Bernoulli's equation.

$$\frac{P_1}{\rho g} + \frac{{V_1}^2}{2g} + Z_1 = \frac{P_2}{\rho g} + \frac{{V_2}^2}{2g} + Z_1 \quad (1.1)$$

However, in order to obtain a significant measurable pressure drop, different types of pressure tappings are used (corner taps, flange taps and D and D/2 taps) in the orifice plate. In comparison to the Venturimeter, the pressure recovery is much less in the case of orifice plate. As per ISO 5167-1 and BS1042 standards [5], the mass flow rate in an orifice plate (Q_m in Kg/s) for a compressible fluid is given by:

$$Q_m = \frac{\epsilon C_d}{\sqrt{1-\beta^4}} \frac{\pi d^2}{4} \sqrt{2\Delta P \rho_1} \quad (1.2)$$

Where: C_d is the discharge coefficient
β is the diameter ratio= d/D
d is the orifice throat diameter, m
D is the upstream pipe diameter, m
ΔP is the differential pressure, Pa
ε is the expansibility factor
ρ_1 is the density at upstream pressure tap location, Kg/m^3

Eqn.1.2 is based on the assumptions that the flow is steady, incompressible, and in viscid flow. However in order to take into account the real fluid effects like viscosity and compressibility, empirical coefficients C_d and ε are introduced in the Eqn.1.2. The discharge coefficient C_d is defined as the ratio of actual flow rate to the theoretical flow rate (calculated on basis of Bernoulli's theorem). The value of C_d depends on the several factors like β, Re, wall roughness, orifice geometry etc. The expansibility factor ε is introduced to take into account to change in density of the fluid as it is passes through the orifice plate for the incompressible fluids ε has a value of unity and for the compressible flow is also less unity. Over the years the orifice plates have been used for metering different fluids (liquid, gas, mixed flow etc...). The performances of these meters in terms of value of discharge coefficient and pressure loss have not been investigated fully by the researchers.

Discharge Coefficient (C_d)

As per ISO 5167 the discharge coefficient for the concentric standard orifice plate assembly is given by following expression

$$C = 0.5959 + 0.0312\beta^{2.1} - 0.1840\beta^8 + 0.0029\beta^{2.5}\left(\frac{10^8}{Re_D}\right)^{0.76} + 0.0900 l_1 \beta^4 (1-\beta^4)^{-1} - 0.0337 l_2' \beta^3 \quad (1.3)$$

Where, $\beta = {}^{d}/_{D}$ is the diameter ratio
Re_D is the Reynolds number
$L_1 = {}^{l_1}/_{D}$ is the distance of the upstream tapping from the upstream face of the plate
$L_2' = {}^{l_2}/_{D}$ is the distance of the downstream tappings from the downstream of the plate

As per ISO-5167-1, the standard dimensions of an orifice plate with flange tappings,

$d > 12.5mm$
$50mm < D < 1000mm$
$0.2 < \beta < 0.75$

$$Re_D > 1260\beta^2 D$$

The above equation is empirical Equations are derived on the bases of experimental data generated over a long period of time. Further the Eqn. 1.3 is also valid if and only if all the specifications in terms of geometry surface finish and installation conditions are satisfied as given in ISO 5167.

Expansibility Factor (ε)

If the fluid is metered with compressible effect, the change in the density takes place as the pressure changes from p_1 to p_2 on passing through the throat section and it is assumed that no transfer of heat occurs and the flow isentropic. The expansibility factor (ε) is calculated by using following empirical formula [ISO 5167 Standard].

$$\epsilon = 1 - (0.351 + 0.256\,\beta^4 + 0.93\beta^8)\left(1 - \left(\frac{p_2}{p_1}\right)^{1/K}\right) \quad (1.4)$$

The Eqn.1.4 is applicable only if $p_2/p_1>0.75$. The uncertainty in the expansibility factor is calculated by following correlation in terms of percent and is given by

$$\Delta\varepsilon = (4\Delta p/p_1)\ \%\ (1.5)$$

II. CFD MODELING AND SIMULATION

CFD modeling is a useful tool to gain an additional insight into the physics of the flow and to understand the test results. The objective of the CFD work is to model the flow using 2D axisymmetric orifice plate geometry to study the flow characteristics that is similar to the practical situation.

The ANSYS FLUENT-14 CFD code is used to model and simulate the flow through orifice plate. The orifice plate geometry was modeled as a 2D-axisymmetric domain using unstructured grid. The dimensions of the geometry were taken from the ISO-5167 and BS1042 standards and no pressure taps were included in the CFD geometry.

In order to validate the CFD methodology, simulation carried out for a standard orifice plate with following dimensions (see Table. 1) and Fig. 2 dimensions of the flow domain used to analysis of flow through standard orifice plate.

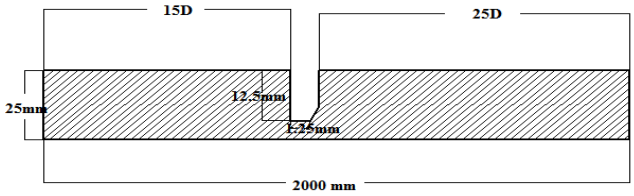

Figure 2, Flow Domains for the Analysis through Orifice Plate

TABLE 1
DIMENSIONS OF THE ORIFICE PLATE

Variables	Values	Units
Diameter of pipe(D)	50	mm
Diameter of throat (d)	25	mm
Diameter Ratio(β)	0.5	---
Upstream pipe length	15D	mm
Downstream pipe length	25D	mm
Thickness of the plate	3	mm
Type of OP beveled	45	Deg.
1mm straight hole followed by 45° beveling		

Fig. 3 shows the CFD mesh used for the orifice plate simulation. The geometry of the model includes 15D of upstream pipe length and a 25D of straight pipe downstream pipe length. The region around orifice plate (±2D) was meshed with very fine grids (see Fig.3), while the upstream and downstream pipe regions were meshed with coarser grids. Boundary layer meshing was used near the wall.

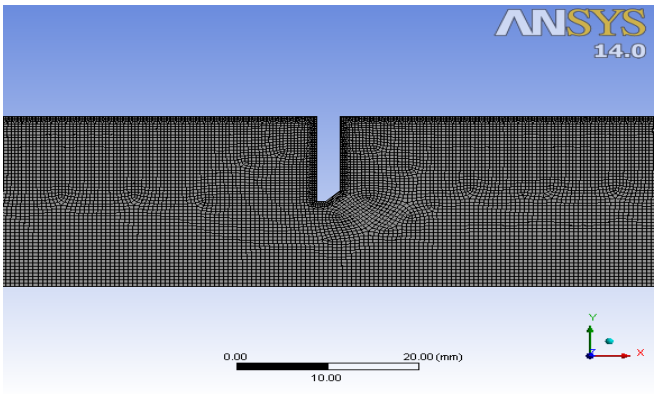

Figure 3. Mesh of Quadrilateral Elements Used For the Orifice Plate for Analysis

III. VALIDATION OF CFD METHODOLOGY

For validation of CFD methodology a standard concentric orifice plate was selected. As per ISO-5167-1, the standard dimensions of an orifice plate with flange tappings.

$$d > 12.5mm$$
$$50mm < D < 1000mm$$
$$0.2 < \beta < 0.75$$
$$Re_D > 1260\beta^2 D$$

Based on the standard limits, an orifice plate with D=50mm and β=0.5 was constructed as a 2D axis symmetric geometry. In the simulation procedure, the process of mesh generation is a very crucial step for better accuracy, stability and economy of prediction. Based on mesh convergence study, a total of 170840 quadrilateral elements were found to be adequate.

The Realizable Spalart Allmars turbulence model with standard wall conditions was selected to model to the turbulent flow field. This choice was based on the computations made with different turbulence models (like K-omega standard, K-omega-SST and K-ε-standard) and the above model gave the best agreement for computed values of C_d with standard values.

For the validation the fluid selected is incompressible liquid with suitable boundary conditions. Velocity at the inlet was specified as 3m/s and at outlet the gauge pressure was set to zero. The density and viscosity of the fluid as chosen to achieve the desired Reynolds number Heat transfer from the wall of the domain was neglected. The solution was computed in the commercial CFD code FLUENT 14, in which the pressure based solver, was selected for this particular case. The computations were made at a Reynolds number of 1×10^5 and the computated value of C_d for flange taps is 0.6041 which is in excellent agreement with the standard value given in ISO-5167(0.6058) and hence CFD methodology was validated. The pressure and velocity contours along with velocity vectors are shown in the Fig. 4. From the contours it is clearly observed that the velocity is increased in the upstream section of the pipe with the corresponding reduction in the pressure, maximum velocity (minimum pressure) is recorded at the throat and velocity reduces when flow passes over the orifice plate section while the pressure recovery occurs in this section. The vector plot shows the flow pattern of the fluid particles inside the orifice plate.

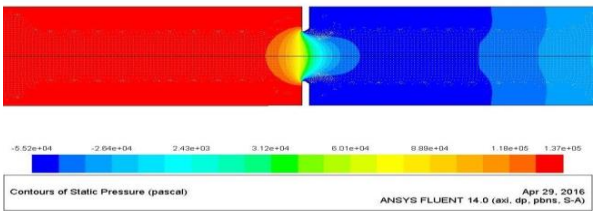

Figure 4(a) Pressure Contours

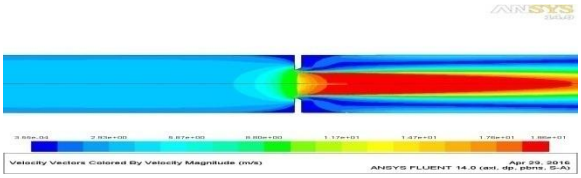

Figure 4(b) Velocity Contours

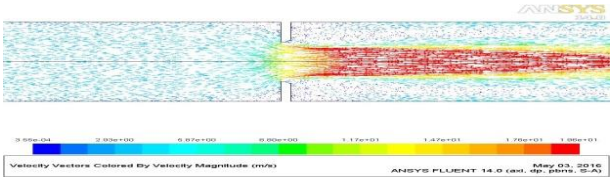

Figure 4(c) Velocity Vector

Figure 4 Contours and Vector Plots for Incompressible Flow through an Standard Orifice Plate (D=50mm, β=0.5)

IV. RESULTS AND DISCUSSION

Having validated the CFD methodology, simulations were performed over a wide range of parameters. Orifice plate discharge coefficients were calculated from the CFD predicted pressure differentials. The simulations were done by keeping constant Reynolds number. Initially the simulation was carried out for a standard concentric orifice plate and the CFD results were validated with the standards. Further the studies were concentrated on compressibility effect, permanent pressure loss coefficient for different orifice plates such as standard orifice plate, quarter circle orifice plate and square edge orifice plate.

A. Compressibility Effect on Standard Concentric Orifice Plate:

Computations have been made for the orifice plate already described (D=50mm, β=0.5 and $Re=1\times10^5$) during the validation. Analyses are made for different diameter ratios in the range 0.3 to 0.7 for the flow of an incompressible fluid at a constant Reynolds number of 1×10^5. The results are tabulated in Table 2. Table 2 also shows the standard values of C_d as per ISO 5167. It is observed that the computed values of Cd are within the uncertainty limits of the standard values. It is observed

that the calculated values of the discharge coefficient are in close agreement with the values given by the code. It is also observed the values of C_d increases with increasing diameter ratio. The same trend is seen in both the CFD computation and ISO 5167 standards. It is to be noted that the standard values given in ISO 5167 are valid for diameter ratios in the range 0.2 to 0.75.

TABLE 2
COMPARISON BETWEEN COMPUTATED AND STANDARD VALUES OF C_d FOR INCOMPRESSIBLE FLOW (D=40mm, Re=1×10^5)

Diameter ratio (β)	C_d (ISO)	C_d (CFD)	Deviation in %	$(C_d)_{uncertainity}$ in%
0.3	0.5990	0.5956	+0.57	±0.6
0.4	0.6019	0.5967	+0.87	±0.6
0.5	0.6058	0.5999	+0.98	±0.6
0.6	0.6115	0.6056	+0.97	±0.6
0.7	0.6152	0.6168	-0.25	±0.7

Computations have been made with gas as working fluid to analyse the effect of compressibility. The gas is assumed to be a perfect gas having a specific heat ratio of 1.4. Further the density of gas at standard temperature and pressure (p= 76cmHg, T=288K) is taken as 1.225 kg/m^3. Energy equations are also solved. Temperature at the inlet is 288K and the adiabatic boundary condition is specified at the outlet. Thus the CFD results give not only the variation in velocity and pressure but also the temperature and density variations are also computed.
The boundary conditions specified for this analysis are constant inlet velocity with gauge pressure at outlet being zero. The computations have been made for different β ratio and constant Reynolds number 1×10^5. For each run, the values of inlet velocity and viscosity are adjusted to obtain the desired Reynolds number. Further these parameters are chosen in a manner by which a wide range of $\Delta p/p_1$ is covered during the computation and the results are tabulated in the Table 3.
The comparison between the computed values of the Discharge coefficient and expansibility factor with the values given in ISO 5167-1 standard for the standard orifice plate with pipe diameter is 40mm and Reynolds number of 1×10^5.

Table 4 gives the codal values of the discharge coefficient for both incompressible and compressible flow further the values of $\Delta p/p_1$are also tabulated it is observed the value of the discharge coefficient for compressible flow is always less than the incompressible flow. The ratio of the two represents the expansibility coefficient. The values of ε calculated from the empirical correlation (ISO 5167-1 standards) are also given in Table 3.

The range of $\Delta p/p_1$ covered in the analysis is from 0.015 to 0.3. As per ISO 5761-1 the values of p_2/p_1 should be greater than 0.75 ($\Delta p/p_1 < 0.25$). The present results are shown even up to $\Delta p/p_1=0.30$ and calculated values of ε agreed with the codal values. The deviations between the two sets of values are of the same order magnitude of uncertainty specified in ISO 5167. Further it is also observed that as $\Delta p/p_1$ increases the value of ε decreases.

TABLE 3
COMPARISON BETWEEN THE COMPUTED AND STANDARD VALUES OF C_d and ε FOR STANDARD ORIFICE PLATE (D=40mm)

β	$\Delta p/p_1$	(C_d) Incom	(C_d) com	ε (CFD)	ε (ISO)
0.3	0.2249	0.5956	0.5769	0.9686	0.9457
0.4	0.1562	0.5967	0.5794	0.9710	0.9639
0.5	0.2571	0.5999	0.5675	0.9460	0.9334
0.6	0.0115	0.6056	0.5968	0.9855	0.9969
0.7	0.3060	0.6168	0.5619	0.9109	0.9117

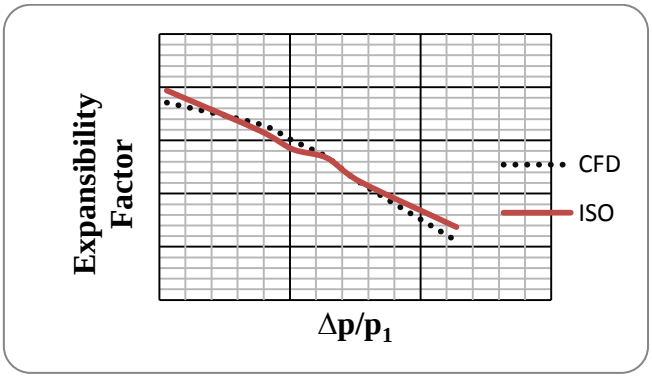

Figure 5. Variation of Expansibility Factor with Pressure Ratio (D=40mm, Re=1×10^5, β=0.3 To 0.7)

Hence the Fig.5 are also shows the excellent agreement between the computated and standard values of ε. Hence the demonstrated that the validated CFD methodology can be used to predict the value of ε of a standard orifice plate under varying conditions. The contours of the

velocity, pressure, density, temperature and velocity vector of the standard orifice plate is as shown in the Fig.6 for the compressible flows.

The Fig. 6(a) shows the pressure contours. It is observed that the maximum pressure occurs when flow approaches in orifice plate and pressure reduces when flow passes over the orifice.

Fig. 6(b) shows the velocity contour. It is observed that the maximum jet velocity developed when fluid passes over the orifice.

Fig. 6(c) shows the velocity vector plot. It is observed that the velocity maximum as jet comes out from the orifice plate. Further a small separated flow region at flow pass over the orifice section where the flow is re-circulating is also clearly seen in the velocity vector plot. Fig.6 (d) shows the density contours. It is observed that the density of the fluid decreases as passes through the orifice plate and then recovers as it flow pass over the orifice section however the recovery is not complete and hence the density of fluid is lower at the outlet as compared to inlet this can attributed the pressure drop in the orifice plate. And Fig.6 (e) shows the temperature contours. It is observed that the temperature of the fluid decreases as passes through the orifice and then recovers as it flow pass over the orifice plate.

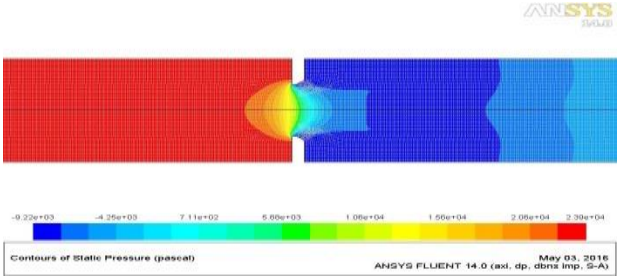

Figure 6(a) Pressure Contours

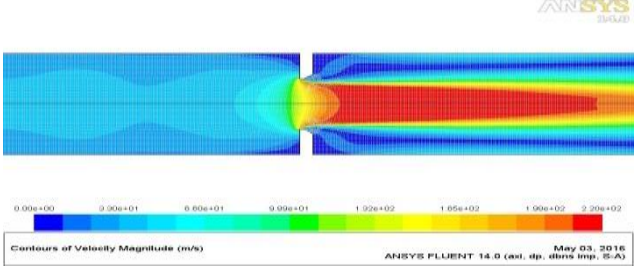

Figure 6(b) Velocity Contours

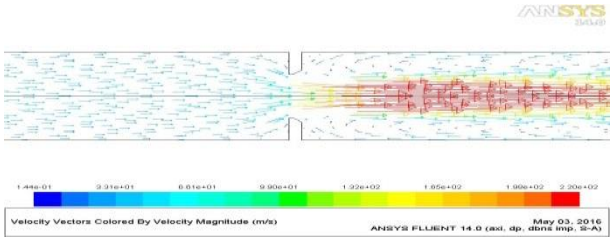

Figure 6(c) Velocity Vector

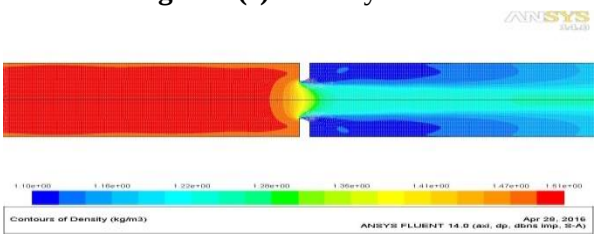

Figure 6(d) Density Contours

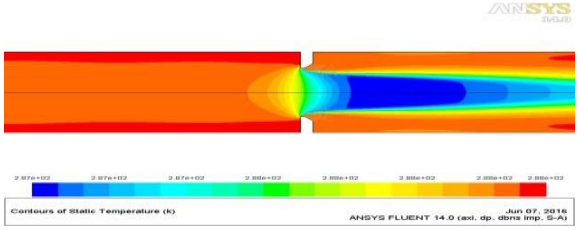

Figure 6(e) Temperature Contours

Figure 6. Contours and Vectors plot for Compressible Flow (β=0.5, D=40mm, Re=1×10^5)

Effect on Permanent Pressure Loss Coefficient

The pressure loss caused by the orifice plate can be determined by the pressure measurement made before and after installation of the orifice plate in a pipe flows. The permanent pressure loss coefficient (C_{PL}) is the ratio of the pressure loss (ΔP^{11}-ΔP^{1}) to the differential pressure loss across the orifice plate. The permanent pressure loss coefficient C_{PL} is given as

$$C_{PL}=\frac{\Delta P''-\Delta P'}{\Delta P_{orifice}} \quad (4.1)$$

Here, Δp^{1} is the pressure difference between the inlet and outlet of the pipe before the installation of the orifice plate. The inlet of the pipe is at -15D and outlet of the pipe is at +25D.

Δp^{11} is the pressure difference under the identical conditions after the installation of orifice plate in the pipe.

$\Delta p_{\text{orifice plate}}$ is the pressure differential between the two pressure taps of the orifice plate.

It is observed ΔP^{11} is always higher than ΔP^{1} . For the purpose of calculating these parameters the upstream and downstream straight lengths of the tube are chosen as 15D and 25D respectively. It is observed from Table 4 that the permanent pressure loss coefficient (C_{PL}) decreases with increasing β ratio. This shows that pressure recovery after the orifice becomes higher as the β ratio increases. It is also seen from the tabulated values that the computed values of C_{PL} are in close agreement with the values calculated on the basis of relation given in ISO 5167. The value of $(C_{PL})_{CFD}$ are in the range of 0.89 to 0.48. Its keeps on decreasing with increasing diameter ratio

TABLE 4
EFFECT OF PERMANENT PRESSURE LOSS COEFFICIENT FOR THE ORIFICE PLATE FOR INCOMPRESSIBLE FLOW (D=40mm)

β	Δp^{11} (Pa)	Δp^{1} (Pa)	Δp_{OP} (Pa)	(C_{PL}) CFD	(C_{PL}) ISO
0.3	3849989	13159	4314889	0.8892	0.8903
0.4	1089990	13159	1335898	0.8062	0.8222
0.5	380398.06	13159	521288	0.7044	0.7296
0.6	151248.65	13159	228880	0.6033	0.6181
0.7	62872.9	13159	103980	0.4781	0.4860

The corresponding values calculated for the compressible flow are tabulated in Table 5

The computation as relevant that the relation given in ISO-5167 accurately predicts the permanent pressure loss due to the orifice plate, it is observed from the tabulated values that the computed values of the C_{PL} and codal values are in good agreement even in the case of compressible fluid flows. The deviations are same order of magnitude as uncertainty in the codal values. Hence it can be conclude that CFD can be used for calculating C_{PL} for both compressible and incompressible fluids.

TABLE 5
EFFECT OF PERMANENT PRESSURE LOSS COEFFICIENT FOR THE STANDARD ORIFICE PLATE FOR COMPRESSIBLE FLOW (D=40mm)

β	Δp^{11} (Pa)	Δp^{1} (Pa)	Δp_{OP} (Pa)	(C_{PL}) CFD	(C_{PL}) ISO
0.3	25215.1	85.84	28162.9	0.8922	0.9040
0.4	14808.0	168.46	17776.8	0.8235	0.8222
0.5	23749.1	555.19	31745.3	0.7306	0.7296
0.6	812.35	85.84	1163.64	0.6242	0.6181
0.7	14283.8	2753.5	23352.5	0.4937	0.4860

B. Effect of Compressibility on Quarter Circle Orifice Plate

The Quarter circle orifice plate is suitable for measurement of flow rate of viscous fluids such as oil. According to BS 1042 standards the value of discharge co efficient and expansibility factor for the quarter circle orifice having some limits which is mentioned in the following sections. The advantage of this orifice plate is that its discharge coefficient remains constant over a wide range of Reynolds number including laminar regime.

According to BS1042 standard the design of Quarter circle orifice meter has to satisfy the following conditions.

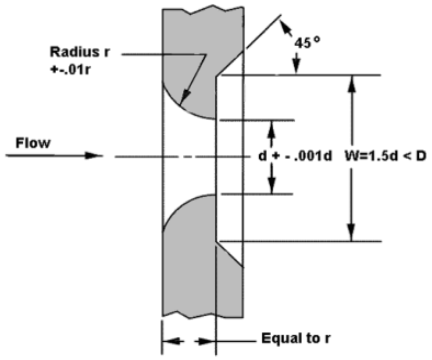

Figure 7. Design of Quarter Circle Orifice

- According to BS 1042 the limits to use for Quarter circle orifice plate are specified below

$d > 15mm$, $D < 500mm$, $0.245 < \beta < 0.6$ and $Re_D < 10^5\beta$

- The discharge coefficient is given by the following equation

$$C = 0.73823 + 0.3309\beta - 1.1615\beta^2 + 1.5084\beta^3$$

- The uncertainty of the discharge co efficient is 2% when $\beta > 0.316$and 2.5 % when $\beta < 0.316$
- The thickness of e in between 2.5mm to 0.1D
- The expansibility factor and uncertainty of expansibility factor for the quarter circle orifice plate is same as specified in the standard orifice plate

In this present work with references of BS 1042 standards, the selection of dimensions for the quarter circle orifice plate for both compressible and incompressible flows is as shown in the Table 6.

TABLE 6
DIMENSIONS OF THE QUARTER CIRCLE ORIFICE PLATE

Variables	Values	Units
Diameter of the pipe	50	mm
Upstream pipe length	15D	mm
Downstream pipe length	25D	mm
Reynolds number	$Re_D < 10^5\beta$	--
Thickness of the plate	5	mm
Length of the pipe	2000	mm

The model created in the CFD is two-dimensional, axis symmetry and mesh of 155674 quadrilateral elements and 157191 nodes are generated in the ANSYS workbench is as shown in the Fig.8 fine mesh is generated across the orifice plate and near the wall boundary layer to obtain the accurate results and also coarse mesh are generated both in upstream and downstream region of the orifice region.

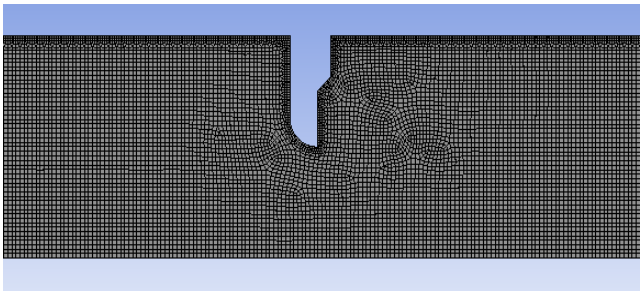

Figure 8. Mesh of Quadrilateral Elements Used For the Quarter Circle Orifice Plate for Analysis

The simulation is carried with turbulent model of Spalart Allmaras with value of Reynolds number being $Re_D < 10^5$ β and pressure based solver is selected for the incompressible flow and density based solver is selected for compressible flow analysis.

The Spalart Allmaras turbulence model with standard wall conditions are selected for simulate the flow domain. The SIMPLE algorithm with the second order upwind is selected for the different iterative process.

The value of the viscosity is chosen to obtain required the value of Reynolds number for incompressible flow and the value of velocity is chosen to obtain the value of Reynolds number for compressible flow, The properties of air are chosen for the compressible fluids whereas water flow properties are chosen for incompressible analysis.

For compressible flow the boundary conditions are velocity at the inlet is specified as 25m/s for diameter ratio 0.5 the outlet gauge pressure zero and the wall is specified as fixed and no slip conditions and also the wall surface is smooth.

The energy equations are required for the solving the compressible flow problems. The boundary conditions of the energy equations is temperature at the inlet is specified as 288K and outlet back flow of the temperature as 288k and the wall is be assumed as adiabatic wall, i.e. there is no heat transfer. Then the solutions are computed with the CFD analysis of FLUENT 14, in which density based solver was selected for this particular compressible flow analysis. Then CFD solutions are compared with the BS1042 standards, for this purpose the expression given for ε for quarter circle orifice plate has used (see eqn.1.3).

TABLE 7
COMPARISON BETWEEN COMPUTATED AND STANDARD VALUES OF C_d FOR INCOMPRESSIBLE FLOW THROUGH QUARTER CIRCLE ORIFICE PLATE (β=0.5, D=50mm)

Reynolds number	C_d (BS1042)	C_d (CFD)	Deviation in %
5000	0.802	0.7995	-0.3117
10000	0.802	0.7976	-0.5486
20000	0.802	0.7973	-0.5860
50000	0.802	0.8038	+0.2244
100000	0.802	0.8155	+1.6832

Table 7 shows the results from the computations made at different Reynolds number for quarter circle orifice plate with D=50mm, β=0.5, the fluid is assumed to incompressible. It is observed the computated values of C_d are in good agreement with the codal values at the all Reynolds number tested in the range 5×10^3 to 1×10^5. It is in testing to note the maximum Reynolds number as per BS1042 is $10^5\times\beta$ which works out to 50000 in this case however even Reynolds number is equal to 10^5. The computated values of C_d agree the value of codal values.

TABLE 8
COMPARISON BETWEEN THE COMPUTED AND STANDARD VALUES OF C_d AND ε FOR QUARTER CIRCLE ORIFICE PLATE (D=50mm)

Reynolds number	C_d (Incom)	C_d (Com)	ε (CFD)	ε (BS1042)	$\Delta p/p_1$
5000	0.7995	0.7891	0.9868	0.9998	0.0003
10000	0.7976	0.7854	0.9847	0.9903	0.0018
20000	0.7973	0.7816	0.9804	0.9986	0.005
50000	0.8038	0.7967	0.9912	0.9924	0.0283
100000	0.8155	0.8027	0.9843	0.9716	0.1055

The computation is made for compressible flows for same orifice plate are shown in Table 8. It is observed that the Cd for the compressible is less for that of incompressible flow for all Reynolds number the agreement between ε_{CFD} and ε_{BS1042} is also reasonable good over an entire range of Reynolds number studied.

The values of the Discharge coefficient for incompressible flow obtained from the CFD simulation and BS1042 standards values are tabulated in the Table 9. From these results the CFD values is very close to the BS1042 standards a value.

It is observed calculated values of the discharge coefficient are in close agreement with the values given by the code. It is observed the values of C_d increases with increasing diameter ratio. The same trend is seen in both the CFD computation and BS 1042 standards.
The deviations between the two sets of values of C_d are within the order of magnitude as the uncertainty specified in the code.

TABLE 9
COMPARISON BETWEEN COMPUTATED AND STANDARD VALUES OF C_d FOR INCOMPRESSIBLE FLOW (D=50mm, Re=1×10^5)

Diameter ratio (β)	Reynolds number	C_d (BS1042)	C_d (CFD)	Deviation in %
0.3	20000	0.774	0.7761	0.27
0.35	25000	0.776	0.7777	0.21
0.4	20000	0.781	0.7843	0.42
0.5	50000	0.802	0.8038	0.22
0.6	100000	0.844	0.8332	1.29

The Comparison between the computed and codal values of C_d and ε for quarter circle orifice plate is listed in the Table 10. The computations have been repeated for the above case using air as working fluid. It is observed that the value of the discharge coefficient for compressible flow is always less than the incompressible flow. The ratio of the two represents the expansibility coefficient. The values of ε are also tabulated in the Table 10.

The values of ε calculated on the basis of equations in BS1042 standards are also given in the Table 10. The deviations in the computed value and BS standard value are observed to be of order of 1.5% in the most of the cases. It is also observed that the input data has been chosen in order to cover a wide range in the parameter $\Delta p/p_1$ since the expansibility factor depends on this parameter. The range of $\Delta p/p_1$ covered in the analysis is from 0.08 to 0.29. As per BS1042 the values of p_2/p_1 should be greater than 0.75 ($\Delta p/p_1 < 0.25$). The present results are shown even up to $\Delta p/p_1$=0.29 and calculated values of ε agreed with the codal values.

TABLE 10
COMPARISON BETWEEN THE COMPUTED AND STANDARD VALUES OF C_d AND ε FOR QUARTER CIRCLE ORIFICE PLATE

β	Re	$\Delta p/p_1$	(C_d) Incom	(C_d) Com	ε (CFD)	ε (ISO)
0.3	20000	0.085	0.776	0.767	0.988	0.980
0.35	25000	0.298	0.777	0.730	0.939	0.926
0.4	20000	0.039	0.784	0.769	0.981	0.990
0.5	50000	0.194	0.803	0.752	0.936	0.949
0.6	100000	0.132	0.833	0.793	0.952	0.964

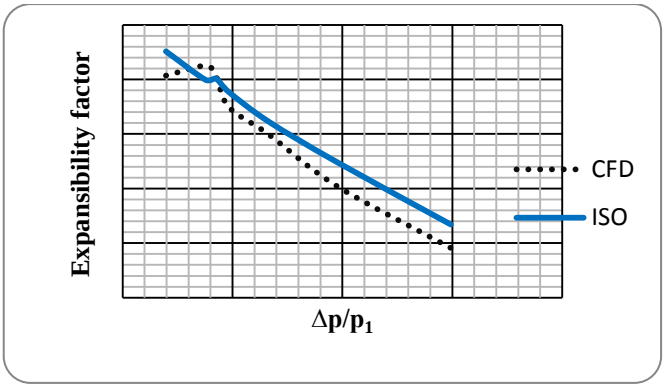

Figure 9. Variation of Expansibility Factor with Pressure Ratio (D=50mm, β=0.3 to 0.6)

Hence Fig.9 also shows the excellent agreement between the computated and standard values of ε. Hence it is demonstrated that the validated CFD methodology can be used to predict the value of ε of a quarter circle orifice plate under varying conditions. The contours of the velocity, pressure, density, temperature and velocity vector of the quarter circle orifice plate is as shown in the Fig.8 for the compressible flows.

Fig. 10(a) shows the pressure contours. It is observed that the maximum pressure occurs when flow approaches in orifice plate and pressure reduces when flow passes over the orifice.

Fig. 10(b) shows the velocity contour. It is observed that the maximum jet velocity developed when fluid passes over the orifice.

Fig. 10(c) shows the velocity vector plot. It is observed that the velocity maximum as jet comes out from the orifice plate. Further a small separated flow region at flow pass over the orifice section where the flow is re-circulating is also clearly seen in the velocity vector plot. F ig.10 (d) shows the density contours. It is observed that the density of the fluid decreases as passes through the orifice plate and then recovers as it flow pass over the orifice section however the recovery is not complete and hence the density of fluid is lower at the outlet as compared to inlet this can attributed the pressure drop in the orifice plate.

Fig.10 (e) shows the temperature contours. It is observed that the temperature of the fluid decreases as passes through the orifice and then recovers as it flow pass over the orifice plate.

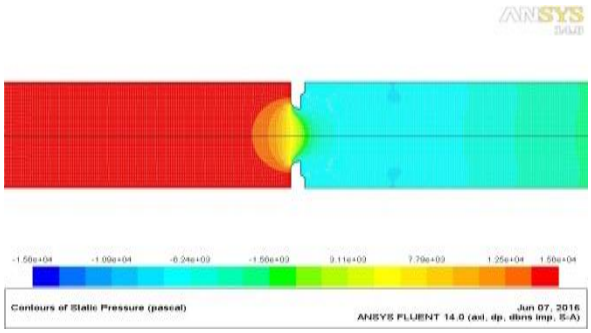

Figure 10(a) Pressure Contours

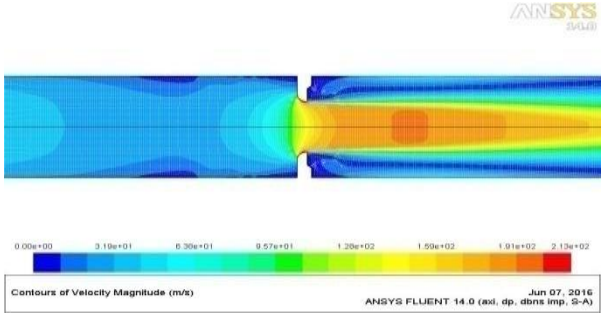

Figure 10(b) Velocity Contours

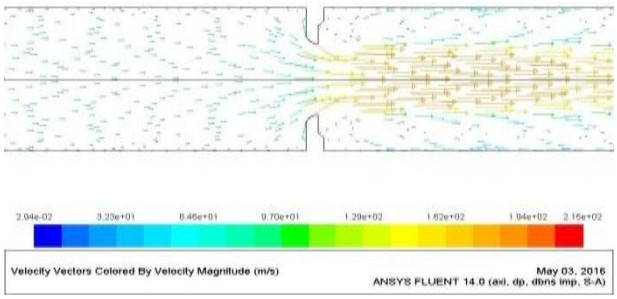

Figure 10(c) Velocity Vector

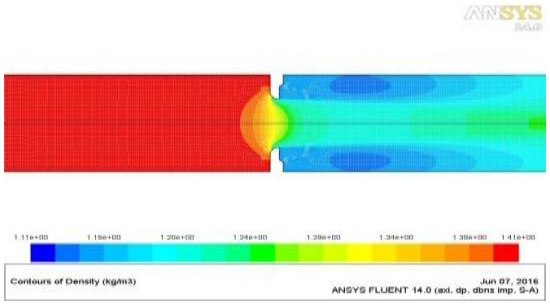

Figure 10(d) Density Contours

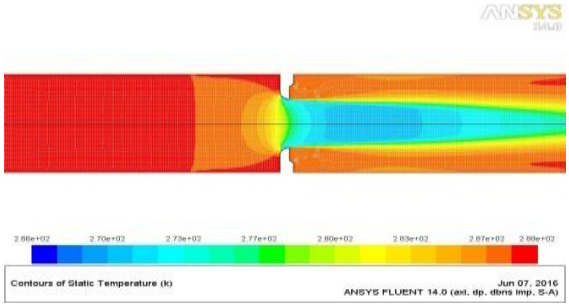

Figure 10(e) Temperature Contours

Figure 10 Contours and Vectors plot for Compressible Flow (β=0.5, D=50mm, Re=50000)

Effect of Permanent Pressure Loss Coefficient

The values of C_{PL} as defined in Eqn.5 have been calculated for both compressible and incompressible flows for various values of different diameter ratios. The results are tabulated in Table 11. It is observed from the tabulated values in Table 11 that for incompressible flow, the permanent pressure loss coefficient (C_{PL}) is dependent on diameter ratio. It is observed Δp^{11} is always higher than Δp^{1}. For the purpose of calculating these parameters the upstream and downstream straight lengths of the tube are chosen as 15D and 25D respectively. It is observed that the permanent pressure loss coefficient C_{PL} decreases with increasing β ratio, this shows that pressure recovery after the orifice becomes higher as the β ratio increases. It is also seen from the tabulated values that the computed values of C_{PL} are in close agreement with the values calculated on the basis of relation given in ISO 5167.

TABLE 11
EFFECT OF PERMANENT PRESSURE LOSS COEFFICIENT FOR THE QUARTER CIRCLE ORIFICE PLATE FOR INCOMPRESSIBLE FLOW

β	Δp^{1} in (Pa)	Δp^{11} in (Pa)	Δp_{OP} in (Pa)	(C_{PL}) CFD	(C_{PL}) BS1042
0.3	793577.4	6085.05	913249	0.8622	0.8692
0.35	402589.5	5829.17	487566	0.8137	0.8252
0.4	217497.4	6085.05	277925.5	0.7606	0.7752
0.5	70822.59	5663.67	104293.5	0.6247	0.6569
0.6	25328.93	3753.19	43454.7	0.4965	0.5086

The corresponding values calculated for the compressible flow are tabulated in the Table 12. It is observed from the tabulated values that the computed values of the C_{PL} and codal values are in good agreement even in the case of compressible fluid flows. The deviations are same order of magnitude as uncertainty in the codal values. Hence it can be concluded that CFD can be used for calculating C_{PL} for both compressible and incompressible fluids.

TABLE 12
EFFECT OF PERMANENT PRESSURE LOSS COEFFICIENT FOR THE QUARTER CIRCLE ORIFICE PLATE FOR COMPRESSIBLE FLOW

β	Δp^{11} in (Pa)	Δp^{1} in (Pa)	Δp_{OP} in (Pa)	(C_{PL}) CFD	(C_{PL}) BS1042
0.3	7401.99	41.665	8690.44	0.8469	0.8717
0.35	31973.86	221.64	39684.35	0.8011	0.8438
0.4	3194.21	68.70	4063.34	0.7691	0.7818
0.5	6841.63	324.25	10353.89	0.6294	0.6923
0.6	5063.45	695.82	7858.82	0.5557	0.5485

V. CONCLUSIONS

CFD modeling and simulations were performed to assess the suitability CFD methodology to analyze the compressibility effects in flow through orifice plates. The results obtained from CFD were used to study the detailed information on orifice plate flow characteristics that could not be easily measured during experimental testing. The validated CFD methodology has been used to analyze the flow through the standard orifice plate and quarter circle orifice plate for both incompressible and compressible flows. The computated values of the C_d, ε and C_{PL} are in close agreement with the values given in ISO 5167 and BS1042 standards. This gives the confidence to predict the characteristics of the orifice plate using CFD even under nonstandard conditions that are not covered in the standard literature. Thus it is also suggested that such computational models can provide an efficient and accurate method for recalibrating flow meters instead of employing costly and time consuming experimental methods.

VI.REFERENCES

[1] Karthik G S , Yogesh Kumar K Y, V Seshadri "*Prediction of Performance Characteristics of Orifice Plate assembly for Non Standard Conditions Using CFD*", Internal National Journal of Engineering And Technology And Technical Research, Issn:2321-0869, Volume-3, Issue-5, May 2015.

[2] W.B.Brower, E.Eisler, K.J.Filkorn, J.Gonenc, C.Plati And J.Stagnitti , "*On The Compressible Flow Through An Orifice*", History : Received January 0.5, 1976; Online October 12,2010A. B. Author, "Title of chapter in the book," in Title of His Published Book, xth ed. City of Publisher, Country if not

[3] Karthik G S (2014), "*CFD analysis Flow through orifice plate Assemblies Used for Specializes Non Standard Working Conditions*", M Tech Thesis, MIT Mysore, VTU 2015

[4] R.Kis, M-Malcho, M-Janovcova, "*A CFD Analysis Of Flow Through A High Pressure Natural Gas Pipeline With An Undeformed And Deformed Orifice Plate*", A T World Academy of Science, Engineering And Technology, International Journal of Mechanical, Aerospace, Industrial, Mechatronic And Manufacturing Engineering.

[5] Indian standard ISO-5167-1, Measurement of fluid flow by means of pressure differential devices (1991).

[6] Diego A.Arias and Timothy A.Shedd, "*CFD Analysis Of Compressible Flow Across A Complex Geometry Venture*" *International Journal Paper.*